BABAR-CONF-08/008
SLAC-PUB-13367

Measurement of Branching Fractions and CP and Isospin Asymmetries in $B \to K^*\gamma$

The BABAR Collaboration

August 14, 2008

Abstract

We present a preliminary analysis of the decays $B^0 \to K^{*0}\gamma$ and $B^+ \to K^{*+}\gamma$ using a sample of 383 million $B\overline{B}$ events collected with the BABAR detector at the PEP-II asymmetric energy B factory. We measure the branching fractions $\mathcal{B}(B^0 \to K^{*0}\gamma) = (4.58 \pm 0.10 \pm 0.16) \times 10^{-5}$ and $\mathcal{B}(B^+ \to K^{*+}\gamma) = (4.73 \pm 0.15 \pm 0.17) \times 10^{-5}$. We measure the direct CP asymmetry to be $-0.043 < \mathcal{A}(B \to K^*\gamma) < 0.025$ and the isospin asymmetry to be $-0.021 < \Delta_{0-} < 0.079$, where the limits are determined at the 90% confidence interval and include both the statistical and systematic uncertainties.

Submitted to the 33rd International Conference on High-Energy Physics, ICHEP 08,
30 July—5 August 2008, Philadelphia, Pennsylvania.

Stanford Linear Accelerator Center, Stanford University, Stanford, CA 94309

Work supported in part by Department of Energy contract DE-AC02-76SF00515.

The *BABAR* Collaboration,

B. Aubert, M. Bona, Y. Karyotakis, J. P. Lees, V. Poireau, E. Prencipe, X. Prudent, V. Tisserand
Laboratoire de Physique des Particules, IN2P3/CNRS et Université de Savoie, F-74941 Annecy-Le-Vieux, France

J. Garra Tico, E. Grauges
Universitat de Barcelona, Facultat de Fisica, Departament ECM, E-08028 Barcelona, Spain

L. Lopez[ab], A. Palano[ab], M. Pappagallo[ab]
INFN Sezione di Bari[a]; Dipartmento di Fisica, Università di Bari[b], I-70126 Bari, Italy

G. Eigen, B. Stugu, L. Sun
University of Bergen, Institute of Physics, N-5007 Bergen, Norway

G. S. Abrams, M. Battaglia, D. N. Brown, R. N. Cahn, R. G. Jacobsen, L. T. Kerth, Yu. G. Kolomensky, G. Lynch, I. L. Osipenkov, M. T. Ronan,[1] K. Tackmann, T. Tanabe
Lawrence Berkeley National Laboratory and University of California, Berkeley, California 94720, USA

C. M. Hawkes, N. Soni, A. T. Watson
University of Birmingham, Birmingham, B15 2TT, United Kingdom

H. Koch, T. Schroeder
Ruhr Universität Bochum, Institut für Experimentalphysik 1, D-44780 Bochum, Germany

D. Walker
University of Bristol, Bristol BS8 1TL, United Kingdom

D. J. Asgeirsson, B. G. Fulsom, C. Hearty, T. S. Mattison, J. A. McKenna
University of British Columbia, Vancouver, British Columbia, Canada V6T 1Z1

M. Barrett, A. Khan
Brunel University, Uxbridge, Middlesex UB8 3PH, United Kingdom

V. E. Blinov, A. D. Bukin, A. R. Buzykaev, V. P. Druzhinin, V. B. Golubev, A. P. Onuchin, S. I. Serednyakov, Yu. I. Skovpen, E. P. Solodov, K. Yu. Todyshev
Budker Institute of Nuclear Physics, Novosibirsk 630090, Russia

M. Bondioli, S. Curry, I. Eschrich, D. Kirkby, A. J. Lankford, P. Lund, M. Mandelkern, E. C. Martin, D. P. Stoker
University of California at Irvine, Irvine, California 92697, USA

S. Abachi, C. Buchanan
University of California at Los Angeles, Los Angeles, California 90024, USA

J. W. Gary, F. Liu, O. Long, B. C. Shen,[1] G. M. Vitug, Z. Yasin, L. Zhang
University of California at Riverside, Riverside, California 92521, USA

[1]Deceased

V. Sharma

University of California at San Diego, La Jolla, California 92093, USA

C. Campagnari, T. M. Hong, D. Kovalskyi, M. A. Mazur, J. D. Richman

University of California at Santa Barbara, Santa Barbara, California 93106, USA

T. W. Beck, A. M. Eisner, C. J. Flacco, C. A. Heusch, J. Kroseberg, W. S. Lockman, A. J. Martinez, T. Schalk, B. A. Schumm, A. Seiden, M. G. Wilson, L. O. Winstrom

University of California at Santa Cruz, Institute for Particle Physics, Santa Cruz, California 95064, USA

C. H. Cheng, D. A. Doll, B. Echenard, F. Fang, D. G. Hitlin, I. Narsky, T. Piatenko, F. C. Porter

California Institute of Technology, Pasadena, California 91125, USA

R. Andreassen, G. Mancinelli, B. T. Meadows, K. Mishra, M. D. Sokoloff

University of Cincinnati, Cincinnati, Ohio 45221, USA

P. C. Bloom, W. T. Ford, A. Gaz, J. F. Hirschauer, M. Nagel, U. Nauenberg, J. G. Smith, K. A. Ulmer, S. R. Wagner

University of Colorado, Boulder, Colorado 80309, USA

R. Ayad,[2] A. Soffer,[3] W. H. Toki, R. J. Wilson

Colorado State University, Fort Collins, Colorado 80523, USA

D. D. Altenburg, E. Feltresi, A. Hauke, H. Jasper, M. Karbach, J. Merkel, A. Petzold, B. Spaan, K. Wacker

Technische Universität Dortmund, Fakultät Physik, D-44221 Dortmund, Germany

M. J. Kobel, W. F. Mader, R. Nogowski, K. R. Schubert, R. Schwierz, A. Volk

Technische Universität Dresden, Institut für Kern- und Teilchenphysik, D-01062 Dresden, Germany

D. Bernard, G. R. Bonneaud, E. Latour, M. Verderi

Laboratoire Leprince-Ringuet, CNRS/IN2P3, Ecole Polytechnique, F-91128 Palaiseau, France

P. J. Clark, S. Playfer, J. E. Watson

University of Edinburgh, Edinburgh EH9 3JZ, United Kingdom

M. Andreotti[ab], D. Bettoni[a], C. Bozzi[a], R. Calabrese[ab], A. Cecchi[ab], G. Cibinetto[ab], P. Franchini[ab], E. Luppi[ab], M. Negrini[ab], A. Petrella[ab], L. Piemontese[a], V. Santoro[ab]

INFN Sezione di Ferrara[a]; Dipartimento di Fisica, Università di Ferrara[b], I-44100 Ferrara, Italy

R. Baldini-Ferroli, A. Calcaterra, R. de Sangro, G. Finocchiaro, S. Pacetti, P. Patteri, I. M. Peruzzi,[4] M. Piccolo, M. Rama, A. Zallo

INFN Laboratori Nazionali di Frascati, I-00044 Frascati, Italy

A. Buzzo[a], R. Contri[ab], M. Lo Vetere[ab], M. M. Macri[a], M. R. Monge[ab], S. Passaggio[a], C. Patrignani[ab], E. Robutti[a], A. Santroni[ab], S. Tosi[ab]

INFN Sezione di Genova[a]; Dipartimento di Fisica, Università di Genova[b], I-16146 Genova, Italy

[2]Now at Temple University, Philadelphia, Pennsylvania 19122, USA
[3]Now at Tel Aviv University, Tel Aviv, 69978, Israel
[4]Also with Università di Perugia, Dipartimento di Fisica, Perugia, Italy

K. S. Chaisanguanthum, M. Morii
Harvard University, Cambridge, Massachusetts 02138, USA

A. Adametz, J. Marks, S. Schenk, U. Uwer
Universität Heidelberg, Physikalisches Institut, Philosophenweg 12, D-69120 Heidelberg, Germany

V. Klose, H. M. Lacker
Humboldt-Universität zu Berlin, Institut für Physik, Newtonstr. 15, D-12489 Berlin, Germany

D. J. Bard, P. D. Dauncey, J. A. Nash, M. Tibbetts
Imperial College London, London, SW7 2AZ, United Kingdom

P. K. Behera, X. Chai, M. J. Charles, U. Mallik
University of Iowa, Iowa City, Iowa 52242, USA

J. Cochran, H. B. Crawley, L. Dong, W. T. Meyer, S. Prell, E. I. Rosenberg, A. E. Rubin
Iowa State University, Ames, Iowa 50011-3160, USA

Y. Y. Gao, A. V. Gritsan, Z. J. Guo, C. K. Lae
Johns Hopkins University, Baltimore, Maryland 21218, USA

N. Arnaud, J. Béquilleux, A. D'Orazio, M. Davier, J. Firmino da Costa, G. Grosdidier, A. Höcker, V. Lepeltier, F. Le Diberder, A. M. Lutz, S. Pruvot, P. Roudeau, M. H. Schune, J. Serrano, V. Sordini,[5] A. Stocchi, G. Wormser
Laboratoire de l'Accélérateur Linéaire, IN2P3/CNRS et Université Paris-Sud 11, Centre Scientifique d'Orsay, B. P. 34, F-91898 Orsay Cedex, France

D. J. Lange, D. M. Wright
Lawrence Livermore National Laboratory, Livermore, California 94550, USA

I. Bingham, J. P. Burke, C. A. Chavez, J. R. Fry, E. Gabathuler, R. Gamet, D. E. Hutchcroft, D. J. Payne, C. Touramanis
University of Liverpool, Liverpool L69 7ZE, United Kingdom

A. J. Bevan, C. K. Clarke, K. A. George, F. Di Lodovico, R. Sacco, M. Sigamani
Queen Mary, University of London, London, E1 4NS, United Kingdom

G. Cowan, H. U. Flaecher, D. A. Hopkins, S. Paramesvaran, F. Salvatore, A. C. Wren
University of London, Royal Holloway and Bedford New College, Egham, Surrey TW20 0EX, United Kingdom

D. N. Brown, C. L. Davis
University of Louisville, Louisville, Kentucky 40292, USA

A. G. Denig M. Fritsch, W. Gradl, G. Schott
Johannes Gutenberg-Universität Mainz, Institut für Kernphysik, D-55099 Mainz, Germany

[5]Also with Università di Roma La Sapienza, I-00185 Roma, Italy

K. E. Alwyn, D. Bailey, R. J. Barlow, Y. M. Chia, C. L. Edgar, G. Jackson, G. D. Lafferty, T. J. West, J. I. Yi

University of Manchester, Manchester M13 9PL, United Kingdom

J. Anderson, C. Chen, A. Jawahery, D. A. Roberts, G. Simi, J. M. Tuggle

University of Maryland, College Park, Maryland 20742, USA

C. Dallapiccola, X. Li, E. Salvati, S. Saremi

University of Massachusetts, Amherst, Massachusetts 01003, USA

R. Cowan, D. Dujmic, P. H. Fisher, G. Sciolla, M. Spitznagel, F. Taylor, R. K. Yamamoto, M. Zhao

Massachusetts Institute of Technology, Laboratory for Nuclear Science, Cambridge, Massachusetts 02139, USA

P. M. Patel, S. H. Robertson

McGill University, Montréal, Québec, Canada H3A 2T8

A. Lazzaro[ab], V. Lombardo[a], F. Palombo[ab]

INFN Sezione di Milano[a]; Dipartimento di Fisica, Università di Milano[b], I-20133 Milano, Italy

J. M. Bauer, L. Cremaldi R. Godang,[6] R. Kroeger, D. A. Sanders, D. J. Summers, H. W. Zhao

University of Mississippi, University, Mississippi 38677, USA

M. Simard, P. Taras, F. B. Viaud

Université de Montréal, Physique des Particules, Montréal, Québec, Canada H3C 3J7

H. Nicholson

Mount Holyoke College, South Hadley, Massachusetts 01075, USA

G. De Nardo[ab], L. Lista[a], D. Monorchio[ab], G. Onorato[ab], C. Sciacca[ab]

INFN Sezione di Napoli[a]; Dipartimento di Scienze Fisiche, Università di Napoli Federico II[b], I-80126 Napoli, Italy

G. Raven, H. L. Snoek

NIKHEF, National Institute for Nuclear Physics and High Energy Physics, NL-1009 DB Amsterdam, The Netherlands

C. P. Jessop, K. J. Knoepfel, J. M. LoSecco, W. F. Wang

University of Notre Dame, Notre Dame, Indiana 46556, USA

G. Benelli, L. A. Corwin, K. Honscheid, H. Kagan, R. Kass, J. P. Morris, A. M. Rahimi, J. J. Regensburger, S. J. Sekula, Q. K. Wong

Ohio State University, Columbus, Ohio 43210, USA

N. L. Blount, J. Brau, R. Frey, O. Igonkina, J. A. Kolb, M. Lu, R. Rahmat, N. B. Sinev, D. Strom, J. Strube, E. Torrence

University of Oregon, Eugene, Oregon 97403, USA

[6]Now at University of South Alabama, Mobile, Alabama 36688, USA

G. Castelli[ab], N. Gagliardi[ab], M. Margoni[ab], M. Morandin[a], M. Posocco[a], M. Rotondo[a], F. Simonetto[ab], R. Stroili[ab], C. Voci[ab]

INFN Sezione di Padova[a]; Dipartimento di Fisica, Università di Padova[b], I-35131 Padova, Italy

P. del Amo Sanchez, E. Ben-Haim, H. Briand, G. Calderini, J. Chauveau, P. David, L. Del Buono, O. Hamon, Ph. Leruste, J. Ocariz, A. Perez, J. Prendki, S. Sitt

Laboratoire de Physique Nucléaire et de Hautes Energies, IN2P3/CNRS, Université Pierre et Marie Curie-Paris6, Université Denis Diderot-Paris7, F-75252 Paris, France

L. Gladney

University of Pennsylvania, Philadelphia, Pennsylvania 19104, USA

M. Biasini[ab], R. Covarelli[ab], E. Manoni[ab],

INFN Sezione di Perugia[a]; Dipartimento di Fisica, Università di Perugia[b], I-06100 Perugia, Italy

C. Angelini[ab], G. Batignani[ab], S. Bettarini[ab], M. Carpinelli[ab],[7] A. Cervelli[ab], F. Forti[ab], M. A. Giorgi[ab], A. Lusiani[ac], G. Marchiori[ab], M. Morganti[ab], N. Neri[ab], E. Paoloni[ab], G. Rizzo[ab], J. J. Walsh[a]

INFN Sezione di Pisa[a]; Dipartimento di Fisica, Università di Pisa[b]; Scuola Normale Superiore di Pisa[c], I-56127 Pisa, Italy

D. Lopes Pegna, C. Lu, J. Olsen, A. J. S. Smith, A. V. Telnov

Princeton University, Princeton, New Jersey 08544, USA

F. Anulli[a], E. Baracchini[ab], G. Cavoto[a], D. del Re[ab], E. Di Marco[ab], R. Faccini[ab], F. Ferrarotto[a], F. Ferroni[ab], M. Gaspero[ab], P. D. Jackson[a], L. Li Gioi[a], M. A. Mazzoni[a], S. Morganti[a], G. Piredda[a], F. Polci[ab], F. Renga[ab], C. Voena[a]

INFN Sezione di Roma[a]; Dipartimento di Fisica, Università di Roma La Sapienza[b], I-00185 Roma, Italy

M. Ebert, T. Hartmann, H. Schröder, R. Waldi

Universität Rostock, D-18051 Rostock, Germany

T. Adye, B. Franek, E. O. Olaiya, F. F. Wilson

Rutherford Appleton Laboratory, Chilton, Didcot, Oxon, OX11 0QX, United Kingdom

S. Emery, M. Escalier, L. Esteve, S. F. Ganzhur, G. Hamel de Monchenault, W. Kozanecki, G. Vasseur, Ch. Yèche, M. Zito

CEA, Irfu, SPP, Centre de Saclay, F-91191 Gif-sur-Yvette, France

X. R. Chen, H. Liu, W. Park, M. V. Purohit, R. M. White, J. R. Wilson

University of South Carolina, Columbia, South Carolina 29208, USA

M. T. Allen, D. Aston, R. Bartoldus, P. Bechtle, J. F. Benitez, R. Cenci, J. P. Coleman, M. R. Convery, J. C. Dingfelder, J. Dorfan, G. P. Dubois-Felsmann, W. Dunwoodie, R. C. Field, A. M. Gabareen, S. J. Gowdy, M. T. Graham, P. Grenier, C. Hast, W. R. Innes, J. Kaminski, M. H. Kelsey, H. Kim, P. Kim, M. L. Kocian, D. W. G. S. Leith, S. Li, B. Lindquist, S. Luitz, V. Luth, H. L. Lynch, D. B. MacFarlane, H. Marsiske, R. Messner, D. R. Muller, H. Neal, S. Nelson, C. P. O'Grady, I. Ofte, A. Perazzo, M. Perl, B. N. Ratcliff, A. Roodman, A. A. Salnikov, R. H. Schindler, J. Schwiening, A. Snyder, D. Su, M. K. Sullivan, K. Suzuki, S. K. Swain, J. M. Thompson, J. Va'vra, A. P. Wagner, M. Weaver, C. A. West, W. J. Wisniewski, M. Wittgen, D. H. Wright, H. W. Wulsin, A. K. Yarritu, K. Yi, C. C. Young, V. Ziegler

Stanford Linear Accelerator Center, Stanford, California 94309, USA

[7]Also with Università di Sassari, Sassari, Italy

P. R. Burchat, A. J. Edwards, S. A. Majewski, T. S. Miyashita, B. A. Petersen, L. Wilden
Stanford University, Stanford, California 94305-4060, USA

S. Ahmed, M. S. Alam, J. A. Ernst, B. Pan, M. A. Saeed, S. B. Zain
State University of New York, Albany, New York 12222, USA

S. M. Spanier, B. J. Wogsland
University of Tennessee, Knoxville, Tennessee 37996, USA

R. Eckmann, J. L. Ritchie, A. M. Ruland, C. J. Schilling, R. F. Schwitters
University of Texas at Austin, Austin, Texas 78712, USA

B. W. Drummond, J. M. Izen, X. C. Lou
University of Texas at Dallas, Richardson, Texas 75083, USA

F. Bianchi[ab], D. Gamba[ab], M. Pelliccioni[ab]
INFN Sezione di Torino[a]; Dipartimento di Fisica Sperimentale, Università di Torino[b], I-10125 Torino, Italy

M. Bomben[ab], L. Bosisio[ab], C. Cartaro[ab], G. Della Ricca[ab], L. Lanceri[ab], L. Vitale[ab]
INFN Sezione di Trieste[a]; Dipartimento di Fisica, Università di Trieste[b], I-34127 Trieste, Italy

V. Azzolini, N. Lopez-March, F. Martinez-Vidal, D. A. Milanes, A. Oyanguren
IFIC, Universitat de Valencia-CSIC, E-46071 Valencia, Spain

J. Albert, Sw. Banerjee, B. Bhuyan, H. H. F. Choi, K. Hamano, R. Kowalewski, M. J. Lewczuk, I. M. Nugent, J. M. Roney, R. J. Sobie
University of Victoria, Victoria, British Columbia, Canada V8W 3P6

T. J. Gershon, P. F. Harrison, J. Ilic, T. E. Latham, G. B. Mohanty
Department of Physics, University of Warwick, Coventry CV4 7AL, United Kingdom

H. R. Band, X. Chen, S. Dasu, K. T. Flood, Y. Pan, M. Pierini, R. Prepost, C. O. Vuosalo, S. L. Wu
University of Wisconsin, Madison, Wisconsin 53706, USA

1 INTRODUCTION

In the Standard Model (SM), the decays $B \to K^*\gamma$ [1] proceed dominantly through one-loop $b \to s\gamma$ electromagnetic penguin transitions. Extensions of the SM predict new high-mass particles that can exist in the loop and alter the SM prediction of the branching fractions. The theoretical predictions of the decay rates [2–5] for $B \to K^*\gamma$ suffer from large hadronic uncertainties, and previous measurements of the branching fractions (Table 1) are more precise than SM estimates. The theoretical estimates and experimental measurements of the branching fractions are in reasonable agreement.

Experimental and theoretical uncertainties are much reduced when considering the CP and isospin asymmetries [9], which are defined by:

$$\mathcal{A} = \frac{\Gamma(\overline{B} \to \overline{K}^*\gamma) - \Gamma(B \to K^*\gamma)}{\Gamma(\overline{B} \to \overline{K}^*\gamma) + \Gamma(B \to K^*\gamma)}, \tag{1}$$

$$\Delta_{0-} = \frac{\Gamma(\overline{B}^0 \to \overline{K}^{*0}\gamma) - \Gamma(B^- \to K^{*-}\gamma)}{\Gamma(\overline{B}^0 \to \overline{K}^{*0}\gamma) + \Gamma(B^- \to K^{*-}\gamma)}. \tag{2}$$

The $K^{*0} \to K_S\pi^0$ mode is excluded from the determination of the CP asymmetry. Being more precise, these quantities allow the SM to be more stringently tested. The SM predictions for the CP asymmetry [10] are on the order of 1%, while the isospin asymmetry [5,11] ranges from 2-10%. The experimental measurements (Table 1) are in good agreement with these predictions. However, new physics models could alter the SM estimates significantly [11–13], and thus precise measurements constrain new physics parameter space.

This note reports on a measurement of the branching fractions $\mathcal{B}(B^0 \to K^{*0}\gamma)$ and $\mathcal{B}(B^+ \to K^{*+}\gamma)$, the isospin asymmetry Δ_{0-}, and the direct CP asymmetries, $\mathcal{A}(B^0 \to K^{*0}\gamma)$ and $\mathcal{A}(B^+ \to K^{*+}\gamma)$.

	CLEOII [6] $9.2 fb^{-1}$	*BABAR* [7] $81.9 fb^{-1}$	*Belle* [8] $78.0 fb^{-1}$
$B^0 \to K^{*0}\gamma$ $(\times 10^{-5})$	$4.55^{+0.72}_{-0.68} \pm 0.34$	$3.92 \pm 0.20 \pm 0.24$	$4.01 \pm 0.21 \pm 0.17$
$B^+ \to K^{*+}\gamma$ $(\times 10^{-5})$	$3.76^{+0.89}_{-0.83} \pm 0.28$	$3.87 \pm 0.28 \pm 0.26$	$4.25 \pm 0.31 \pm 0.24$
$\mathcal{A}$	$+0.08 \pm 0.13 \pm 0.03$	$-0.013 \pm 0.036 \pm 0.010$	$-0.015 \pm 0.044 \pm 0.012$
Δ_{0-}	N/A	$+0.050 \pm 0.045 \pm 0.028 \pm 0.024$	$+0.012 \pm 0.044 \pm 0.026$

Table 1: Previous measurements of the branching ratios and asymmetries. The first and second errors are statistical and systematic respectively. The last error on the isospin asymmetry for the *BABAR* measurement refers to the error on the production ratio of charged to neutral B events, $R^{+/0} \equiv \Gamma(\Upsilon(4S) \to B^+B^-)/\Gamma(\Upsilon(4S) \to B^0\bar{B}^0)$.

2 THE *BABAR* DETECTOR AND DATASET

We use a data sample containing 383 million $B\overline{B}$ events, corresponding to an integrated luminosity of 347 fb^{-1} collected at the $\Upsilon(4S)$ resonance, taken with the *BABAR* detector at the PEP-II

asymmetric-energy e^+e^- collider located at the Stanford Linear Accelerator Center (SLAC). These results supersede the previous *BABAR* measurements [7].

The *BABAR* detector is described in Ref. [14]. Two components that are especially important for this analysis are the CsI Electromagnetic Calorimeter (EMC), used to identify and measure photon energies, and the DIRC Cherenkov detector, used to identify charged particles.

3 ANALYSIS METHOD

We reconstruct $B^0 \to K^{*0}\gamma$ using the modes $K^{*0} \to K^+\pi^-$ and $K^{*0} \to K_S\pi^0$, and $B^+ \to K^{*+}\gamma$ using the decay modes $K^{*+} \to K^+\pi^0$ and $K^{*+} \to K_S\pi^+$. A high energy photon is combined with each vector meson.

The dominant source of background is continuum events ($e^+e^- \to q\bar{q}$, with $q = u, d, s, c$) that contain a high-energy photon from π^0 or η decay. The remaining background consists primarily of initial-state radiation (ISR) processes, and higher-multiplicity $b \to s\gamma$ decays, where one or more particles has not been reconstructed. In addition, the decays of $B \to K^*\gamma$ can enter the signal selection by mis-reconstructing a similar mode. For example, the decay $B \to K^*\gamma(K^{*+} \to K^+\pi^0)$ provides background for the mode $B \to K^*\gamma(K^{*0} \to K^+\pi^-)$ by not correctly reconstructing the π meson. For each signal decay mode, selection requirements described below have been optimized for maximum statistical sensitivity with an assumed signal branching fraction of 4.0×10^{-5} [7].

Photon candidates are identified as localized energy deposits in the EMC that are not associated with any charged track. The primary photon candidate is required to have a center-of-mass (CM) energy between 1.5 and 3.5 GeV, to be well-isolated and have a shower shape consistent with an individual photon [15]. In order to veto photons from π^0 and η decays, we form photon pairs composed of the signal photon candidate and all other photon candidates in the event. We then reject primary photon candidates consistent with coming from a π^0 or η decay based on a likelihood ratio that uses the energy of the partner photon, and the invariant mass of the pair.

The charged tracks must be well-reconstructed in the drift chamber, and are required to be consistent with coming from the e^+ e^- interaction region. They are identified as K or π mesons by the Cherenkov angle with respect to track direction, as well as by energy loss of the track (dE/dx). The K_S candidates are reconstructed from two oppositely charged tracks that come from a common vertex. We require the invariant mass of the pair to be $0.49 < m_{\pi^+\pi^-} < 0.52$ GeV/c^2($0.48 < m_{\pi^+\pi^-} < 0.52$ GeV/c^2) and have a K_S flight length significance requirement of 9.3(10) for the $K^{*0} \to K_S\pi^0(K^{*+} \to K_S\pi^+)$ mode.

We form π^0 candidates by combining two photons (excluding the primary photon candidate) in the event, each of which has an energy greater than 30 MeV in the laboratory frame. We require the invariant mass of the pair to be $0.112 < m_{\gamma\gamma} < 0.15$ GeV/c^2 and $0.112 < m_{\gamma\gamma} < 0.15$ GeV/c^2 for the $K^{*0} \to K_S\pi^0$ and $K^{*+} \to K^+\pi^0$ modes respectively. In order to refine the π^0 three momentum vector, we perform a mass-constrained fit of the two photons.

We combine the reconstructed K or π mesons to form K^* candidates. We require the invariant mass of the pair to satisfy $0.78 < m_{K^+\pi^-} < 1.1$ GeV/c^2, $0.82 < m_{K_S\pi^0} < 1.0$ GeV/c^2, $0.79 < m_{K^+\pi^0} < 1.0$ GeV/c^2, and $0.79 < m_{K_S\pi^+} < 1.0$ GeV/c^2. The charged track pairs are required to originate from a common vertex consistent with the e^+e^- collision region.

We combine the K^* and high-energy photon candidates to form B candidates. We define in the CM frame (the asterisk denotes the CM quantity) $\Delta E \equiv E^*_B - E^*_{\text{beam}}$, where E^*_B is the energy of the B meson candidate and E^*_{beam} is the beam energy. We also define the beam-energy-substituted

mass $m_{\rm ES} \equiv \sqrt{E^{*2}_{\rm beam} - {\rm p}^{*2}_B}$, where ${\rm p}^*_B$ is the momentum of the B candidate. In addition, we consider the helicity angle θ_H of the K^*, defined as the angle between one of the daughters of the K^* meson and the B candidate in the K^* rest frame. Signal events have ΔE close to zero with a resolution of approximately 50 MeV, and an $m_{\rm ES}$ distribution centered at the mass of the B meson with a resolution of 3 MeV/c^2. Since the K^* recoils against a photon, it has a $\cos\theta_H$ distribution of $\sin^2\theta$. We only consider candidates in the ranges $-0.3 < \Delta E < 0.3$ GeV, $m_{\rm ES} > 5.22$ GeV/c^2, and $|\cos\theta_H| < 0.75$. The latter selection is to reject background such as $B \to K^*\eta$ and $B \to K^*\pi^0$, which are distributed as $\cos^2\theta$ in $\cos\theta_H$. To ensure the events are properly reconstructed, we apply a selection criterion to the separation (and its uncertainty) along the beam axis between the B meson candidate and the rest of the event (ROE). The ROE is defined as all charged tracks and neutral energy deposits in the calorimeter that are not used to reconstruct the B candidate.

In order to reject continuum background, we combine 13 variables into a neural network (NN) [16]. One class of these variables exploits the topological differences between spherical signal events and jet-like continuum events by considering information from the B meson candidate and the ROE. The other class exploits the difference in particle production mechanisms between B meson decays and continuum events. The discriminating variables are described in Ref. [17]. Each mode has a separately trained neural network. The output of this network peaks at a value of one for signal-like events. We select events with a criterion on this output that is optimized for maximum statistical sensitivity. To validate the neural network, we use a $B \to D\pi$ control sample.

After applying all the selection criteria, we select the best candidate in each event by choosing the candidate with the reconstructed K^* mass closest to the nominal mass. On average, across all four modes, there are approximately 1.1 candidates per event in signal events.

We perform an unbinned maximum likelihood fit to extract the signal yield, constructing a separate fit for each mode. We use three observables ($m_{\rm ES}$, ΔE, and $\cos\theta_H$) for each candidate event and assume three hypotheses (signal, continuum, and $B\overline{B}$) from which the candidate can originate. All $B\overline{B}$ background is included in the $B\overline{B}$ component. The use of $\cos\theta_H$ suppresses the $B\overline{B}$ background. Since the correlations among the three dimensions are small, we use uncorrelated probability distribution functions (PDF) to construct the likelihood function. The correction to this method is determined in section 4. The likelihood function is:

$$\mathcal{L} = \exp\left(-\sum_{i=1}^{M} n_i\right) \cdot \left(\prod_{j=1}^{N}\left[\sum_{i=1}^{M} n_i \mathcal{P}_i(\vec{x}_j;\ \vec{\alpha}_i)\right]\right)$$

where N is the number of events, M is the number of hypotheses, n_i represents the yield of a particular hypothesis, $\mathcal{P}_i(\vec{x}_j;\vec{\alpha}_i)$ is the product of one-dimensional PDFs over the three dimensions, $\vec{x}_j = (m_{\rm ES}, \Delta E, \cos\theta_H)$, and the $\vec{\alpha}_i$ represent the fit parameters.

The signal $m_{\rm ES}$ PDF for the $K^{*0} \to K^+\pi^-$ and $K^{*+} \to K_S\pi^+$ modes is parameterized as

$$f(x) = \exp\left[\frac{-(x-\mu)^2}{2\sigma^2_{L,R} + \alpha_{L,R}(x-\mu)^2}\right], \qquad (3)$$

where μ is the peak position of the distribution, $\sigma_{L,R}$ are the widths to the left and right of the peak, and $\alpha_{L,R}$ are a measure of the tails to the left and right of the peak, respectively. We constrain $\sigma_L = \sigma_R$, and fix $\alpha_{L,R}$ to the values obtained from Monte Carlo (MC) simulation [18]. For the $K^{*0} \to K_S\pi^0$ and $K^{*+} \to K^+\pi^0$ modes, the signal $m_{\rm ES}$ distribution is described by a Crystal Ball function [19]. The Crystal Ball function has a single tail parameter, α, which we fix to the value

determined from MC. For each mode, the signal ΔE distribution is described by the same function in Eq. 3, but with different values for the parameters. However, we allow σ_L and σ_R to float independently, but still fix the values of $\alpha_{L,R}$ to MC. For all components, the $\cos\theta_H$ distribution is modeled by a low order polynomial, which is fixed to the MC values. For the continuum hypothesis, the $m_{\rm ES}$ PDF is parameterized by an ARGUS function [20], with its shape parameter floating in the fit. The continuum ΔE shape is modeled by a low order polynomial with its parameters floating in the fit. Various functional forms are used to describe the $B\overline{B}$ background, all parameters of which are taken from MC simulation and held fixed.

The CP asymmetry $\mathcal{A}$ parameter is measured in the three "self-tagging" modes: $K^{*0} \to K^+\pi^-$, $K^{*+} \to K^+\pi^0$ and $K^{*+} \to K_S\pi^+$. The fit is accomplished by performing a simultaneous fit to the two flavor sub-samples (K^* and $\overline{K^*}$) in each mode. All shape parameters are assumed to be flavor independent and the $\mathcal{A}$ of each component is floated in the fit.

Figures 1 through 4 show the projections of the likelihood fit to data. For each projection, signal region cuts ($5.27 < m_{\rm ES} < 5.29$ GeV/c^2, $-0.2 < \Delta E < 0.1$ GeV) have been applied, except the $m_{\rm ES}$ selection is not applied to the $m_{\rm ES}$ distribution and similarly for ΔE. The asymmetry of the signal component of the $\cos\theta_H$ distributions is due to mis-reconstructed signal candidates. Table 2 shows the results for the branching fractions and CP asymmetry, where the sign of $\mathcal{A}$ is defined by Eq. 1.

Mode	$\epsilon(\%)$	N_S	$\mathcal{B}(\times 10^{-5})$	$\mathcal{A}$
$K^+\pi^-$	20.6±0.7	2394.1±55.6	$4.55 \pm 0.11 \pm 0.16$	$-0.023 \pm 0.022 \pm 0.011$
$K_s\pi^0$	11.7±0.8	256.0 ±20.6	$5.01 \pm 0.40 \pm 0.37$	N/A
$K^+\pi^0$	13.7±0.7	872.7±37.6	$5.05 \pm 0.22 \pm 0.27$	$+0.033 \pm 0.039 \pm 0.011$
$K_s\pi^+$	18.8±0.7	759.1±33.8	$4.56 \pm 0.20 \pm 0.17$	$-0.006 \pm 0.041 \pm 0.011$
$B^0 \to K^{*0}\gamma$			$4.58 \pm 0.10 \pm 0.16$	
$B^+ \to K^{*+}\gamma$			$4.73 \pm 0.15 \pm 0.17$	
$B \to K^*\gamma$				$-0.009 \pm 0.017 \pm 0.011$

Table 2: The signal reconstruction efficiency ϵ, the fitted signal yield N_S, branching fraction $\mathcal{B}$, and CP asymmetry ($\mathcal{A}$) for each decay mode. The signal efficiencies have been corrected for differences between the selection efficiency in data and MC. Errors are statistical and systematic, with the exception of ϵ and N_S, which have only systematic and statistical errors respectively. Also shown are the combined branching fractions and CP asymmetry.

4 SYSTEMATIC ERROR STUDIES

Table 3 lists the sources of systematic uncertainty for all four modes. These are associated with the signal reconstruction efficiency, modeling of the $B\overline{B}$ background, and the choice of fixed parameters of the fit PDFs. The "Photon selection" systematic error is a combination of the photon efficiency, the isolation criteria, and the shower shape selection. For the Neural Net and the π^0/η veto, we use a $B \to D\pi$ control sample to determine the systematic error. The "Fit Model" systematic error is a combination of incorporating uncertainties due to our imperfect knowledge of the normalization and shape of the inclusive $B \to X_s\gamma$ spectra, and the choice of fixed parameters. We also perform a series of experiments in which we select signal events from MC simulation and combine them with events

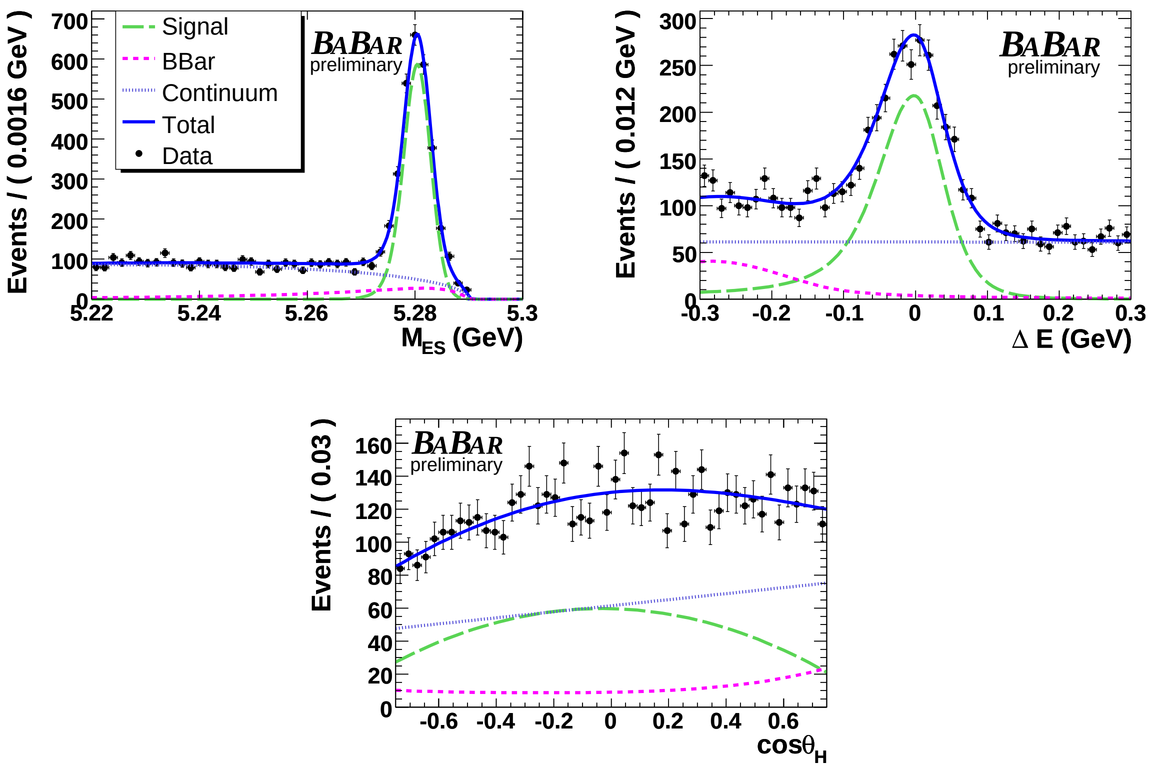

Figure 1: $K^{*0} \to K^+\pi^-$ projection plots of the full fit to data. The daughter of the K^* used to determine the helicity angle is the K meson.

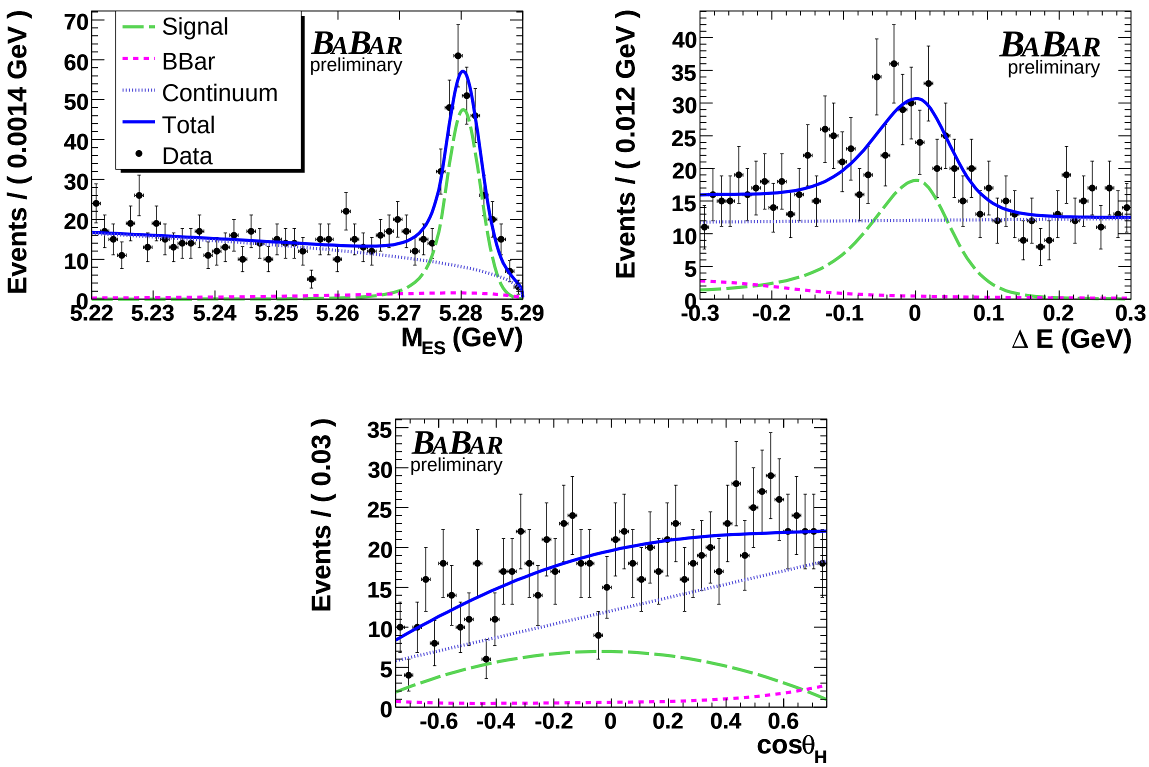

Figure 2: $K^{*0} \to K_S\pi^0$ projection plots of the full fit to data. The daughter of the K^* used to determine the helicity angle is the K_S.

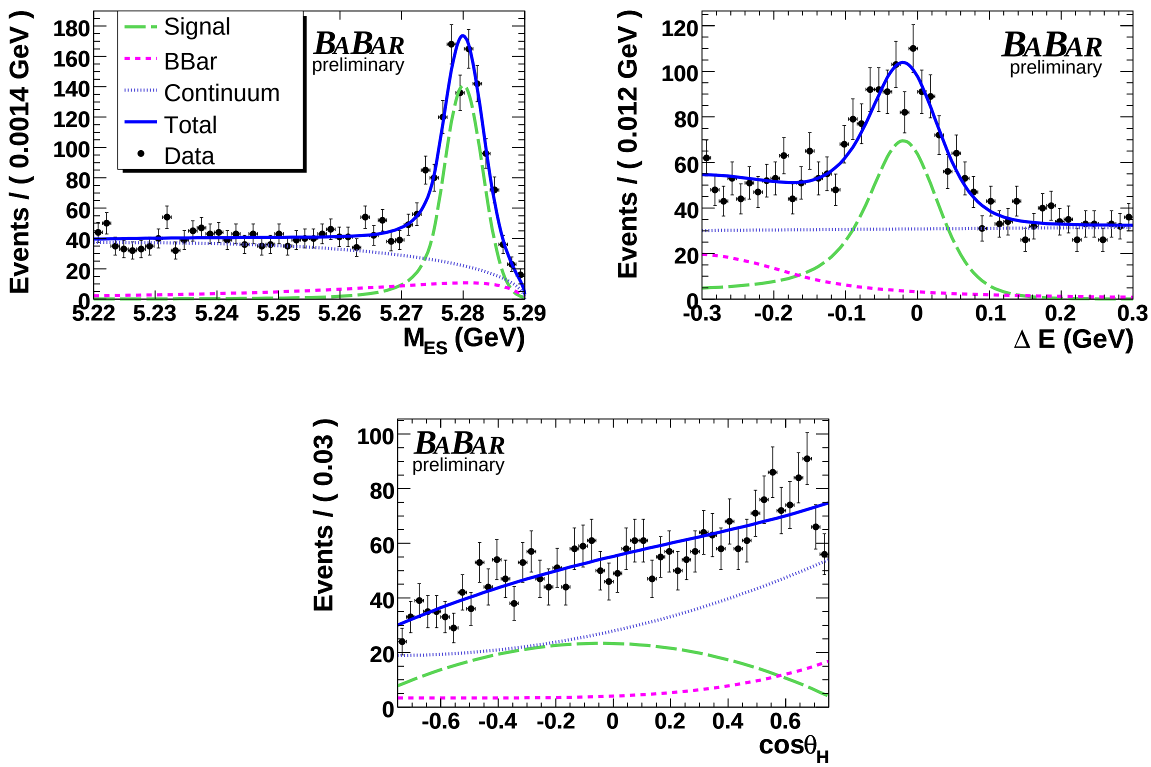

Figure 3: $K^{*+} \to K^+\pi^0$ projection plots of the full fit to data. The daughter of the K^* used to determine the helicity angle is the K^+.

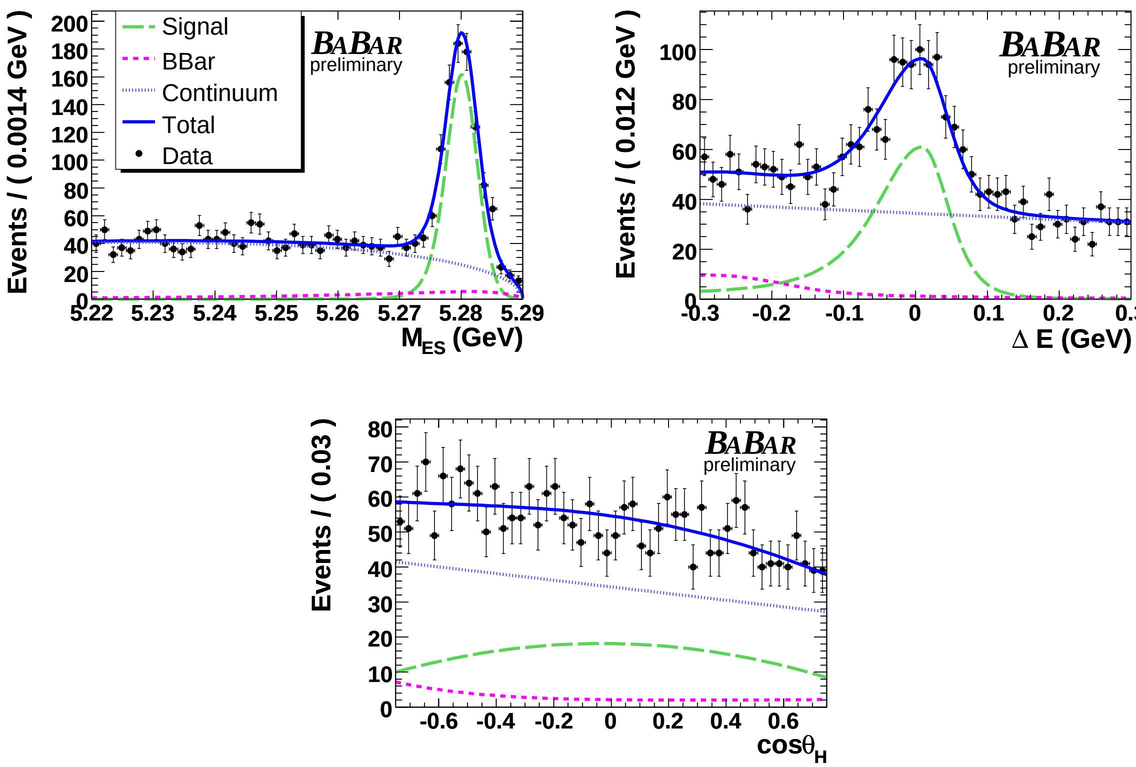

Figure 4: $K^{*+} \rightarrow K_S\pi^+$ projection plots of the full fit to data. The daughter of the K^* used to determine the helicity angle is the π meson.

from background generated using PDFs from the fit. The bias resulting from correlations among the three dimensions, or the PDFs incorrectly modeling the signal distribution can be determined using this procedure. The "Signal PDF bias" systematic error results from these series of experiments. Associated with all of the systematic uncertainties is a correction factor, which is a ratio between the estimated efficiency in data and the corresponding efficiency in MC. The corrections are 0.953, 0.897, 0.919, and 0.936 for the $K^{*0} \to K^+\pi^-$, $K^{*0} \to K_S\pi^0$, $K^{*+} \to K^+\pi^0$, and $K^{*+} \to K_S\pi^+$ modes respectively. We use this factor to correct the MC reconstruction efficiency.

The systematics of the $\mathcal{A}$ measurement were studied in detail in Reference [15]. They were found to be due to uncertainties in the hadronic cross section asymmetry and to reconstruction asymmetries. Here, we simply adopt the value 1.1%, which is a conservative estimate due to reconstruction improvements.

Table 3: Systematic errors (in %) of the branching fractions.

Mode	$K^{*0} \to K^+\pi^-$	$K^{*0} \to K_S\pi^0$	$K^{*+} \to K^+\pi^0$	$K^{*+} \to K_S\pi^+$
$B\overline{B}$ sample size	1.1	1.1	1.1	1.1
Tracking efficiency	1.2	-	0.6	0.8
Particle identification	0.6	-	0.6	0.2
Photon selection	2.2	2.2	2.2	2.2
π^0 reconstruction	3.0	-	3.0	-
π^0 and η veto	1.0	1.0	1.0	1.0
K_S reconstruction	-	0.7	-	0.7
Neural Net efficiency	1.5	1.0	1.0	1.0
Fit Model	0.7	5.3	2.9	1.6
Signal PDF bias	0.9	2.2	1.6	1.4
Sum in quadrature	3.5	7.1	5.3	3.7

5 RESULTS

For the branching fraction calculation, we assume the production ratio, $R^{+/0}$, is unity. $R^{+/0}$ is defined as

$$R^{+/0} = \frac{\Gamma(\Upsilon(4s) \to B^+B^-)}{\Gamma(\Upsilon(4s) \to B^0\bar{B}^0)}.$$

The measured branching fractions are shown in Table 2. The combined branching fractions are calculated from the sub-modes using the method of least squares, taking into account correlated systematic errors.

To calculate the isospin asymmetry Δ_{0-}, we combine the branching fractions, the ratio of the B^+ and B^0 lifetime τ_+/τ_0, and the production ratio $R^{+/0}$ according to

$$\Delta_{0-} = \frac{1}{2}(IR^{+/0}\frac{\tau^+}{\tau^0} - 1), \tag{4}$$

where I is

$$I = \frac{\mathcal{B}(B^0 \to K^{*0}\gamma)}{\mathcal{B}(B^{*-} \to K^{*-}\gamma)},$$

to obtain the isospin asymmetry

$$\Delta_{0-} = 0.029 \pm 0.019 \pm 0.016 \pm 0.018.$$

The first and second errors are statistical and systematic, respectively. The last error comes from the error on the production ratio, and we have used $\tau_+/\tau_0 = 1.071 \pm 0.009$ [21], $R^{+/0} = 1.020 \pm .034$ [22]. In addition, to obtain Eq. 4, we have used the approximation that I, $R^{+/0}$, and τ_+/τ_0 are all close to unity. The 90% confidence interval for Δ_{0-} including systematic uncertainties is

$$-0.021 < \Delta_{0-} < 0.079.$$

The corresponding time-integrated CP asymmetry (table 2) is

$$\mathcal{A} = -0.009 \pm 0.017 \pm 0.011,$$

while the 90% confidence interval for $\mathcal{A}$ is

$$-0.043 < \mathcal{A} < 0.025.$$

The combined asymmetries are calculated using the same method as the branching fractions.

To ensure that we are measuring real K^* mesons in data, we widen the K^* mass selection to be $0.7 < m_{K\pi} < 1.1$ GeV/c^2, refit the data, and make an sPlot [23] of the K^* mass. We then fit a relativistic P-wave Breit-Wigner line shape to the sPlot. This is shown in Figure 5. We combine the measurements of mean of the K^* mass and the width for the charged and neutral mesons separately to obtain the results in Table 4. The results are consistent with the PDG values.

	Data		PDG Value	
K^* meson	m (MeV)	Γ(MeV)	m (MeV)	Γ(MeV)
K^{*0}	894.34$\pm$ .63	47.1$\pm$ 1.4	896.00$\pm$ .25	50.3$\pm$ 0.6
K^{*+}	892.88$\pm$ .80	46.7$\pm$ 1.8	891.66$\pm$ .26	50.8$\pm$ 0.9

Table 4: The combined results of the fits to the $m_{K\pi}$ spectrum shown in Figure 5. Also shown are the PDG values.

6 CONCLUSIONS

We present a preliminary measurement of the branching fractions $\mathcal{B}(B^0 \to K^{*0}\gamma) = (4.58 \pm 0.10 \pm 0.16) \times 10^{-5}$ and $\mathcal{B}(B^+ \to K^{*+}\gamma) = (4.73 \pm 0.15 \pm 0.17) \times 10^{-5}$. We use these results to calculate the isospin asymmetry at the 90% confidence interval to be $-0.021 < \Delta_{0-} < 0.079$. We also present a preliminary measurement of the time-integrated CP asymmetry at the 90% confidence interval to be $-0.043 < \mathcal{A} < 0.025$. These results are all improvements over previous measurements, as well as being consistent with SM expectations.

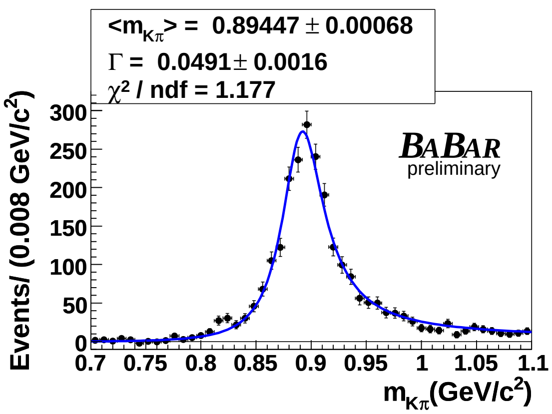

(a) $K^{*0} \to K^+\pi^-$ mode

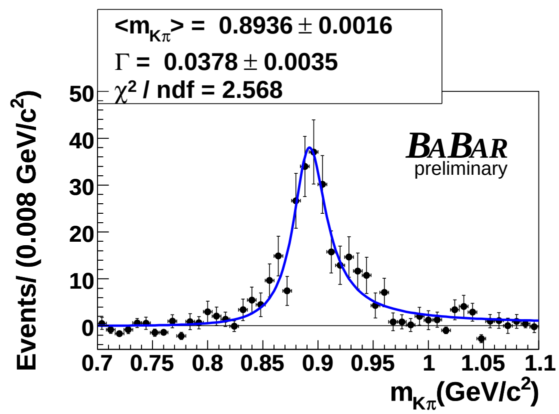

(b) $K^{*0} \to K_S\pi^0$ mode

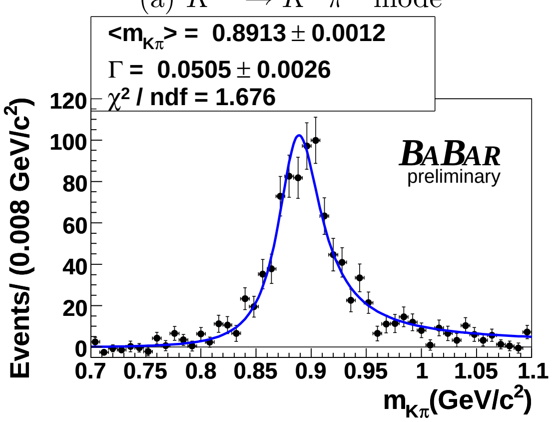

(c) $K^{*+} \to K^+\pi^0$ mode

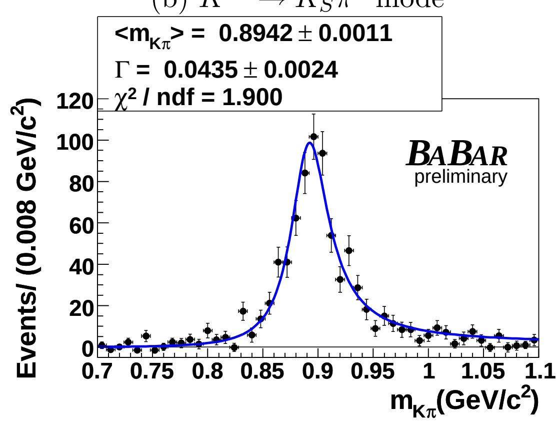

(d) $K^{*+} \to K_S\pi^+$ mode

Figure 5: Relativistic P-wave Breit-Wigner line shape fit to the $K\pi$ invariant mass distribution of the sPlot of data for the a) $K^{*0} \to K^+\pi^-$, b) $K^{*0} \to K_S\pi^0$, c) $K^{*+} \to K^+\pi^0$, and d) $K^{*+} \to K_S\pi^+$ modes.

7 ACKNOWLEDGMENTS

We are grateful for the extraordinary contributions of our PEP-II colleagues in achieving the excellent luminosity and machine conditions that have made this work possible. The success of this project also relies critically on the expertise and dedication of the computing organizations that support *BABAR*. The collaborating institutions wish to thank SLAC for its support and the kind hospitality extended to them. This work is supported by the US Department of Energy and National Science Foundation, the Natural Sciences and Engineering Research Council (Canada), the Commissariat à l'Energie Atomique and Institut National de Physique Nucléaire et de Physique des Particules (France), the Bundesministerium für Bildung und Forschung and Deutsche Forschungsgemeinschaft (Germany), the Istituto Nazionale di Fisica Nucleare (Italy), the Foundation for Fundamental Research on Matter (The Netherlands), the Research Council of Norway, the Ministry of Education and Science of the Russian Federation, Ministerio de Educación y Ciencia (Spain), and the Science and Technology Facilities Council (United Kingdom). Individuals have received support from the Marie-Curie IEF program (European Union) and the A. P. Sloan Foundation.

References

[1] K^* refers to the $K^*(892)$ resonance throughout this paper.

[2] A. Ali and A. Y. Parkhomenko, Eur. Phys. Jour. C **23**, 89 (2002).

[3] S. W. Bosch and G. Buchalla Nucl. Phys. B **621**, 459 (2002).

[4] M. Beneke and T. Feldmann D. and Seidel, Nucl. Phys. B **612**, 25 (2001).

[5] M. Matsumori and A.I. Sanda and Y.-Y. Keum, Physical Review D **72**, 014013 (2005).

[6] T. E. Coan *et al.*, Phys. Rev. Lett. **84**, 5283 (2000).

[7] B. Aubert *et al.*, Physical Review D **70**, 112006 (2004).

[8] M. Nakao *et al.*, Physical Review **69**, 112001 (2004).

[9] Charge conjugate modes are implied throughout, except for the CP asymmetry.

[10] C. Greub and H. Simma D. Wyler, Nucl. Phys. B **434**, 39 (1995).

[11] A. L. Kagan and M. Neubert, Phys. Lett. B **539**, 227 (2002).

[12] M. R. Ahmady and F. Mahmoudi, Physical Review D **75**, 015007 (2007).

[13] C. Dariescu and M. Dariescu, arXiv:0710.3819 [hep-ph].

[14] B. Aubert *et al.*, Nucl. Instrum. Methods A **479**, 1 (2002).

[15] B. Aubert *et al.*, Phys. Rev. Lett. **88**, 101805 (2002).

[16] S. Haykin, *Neural Networks: A Comprehensive Foundation.* Macmillan College Publishing Company,, Inc., Englewood Cliffs, NF, 1994.

[17] B. Aubert *et al.*, Phys. Rev. Lett. **98**, 151802 (2007).

[18] S. Agostinelli *et al.*, Nucl. Instrum. Methods A **506**, 250 (2003).

[19] Oreglia, M. J., Ph.D Thesis, SLAC-236 (1980), Gaiser, J. E., Ph.D. Thesis, SLAC-255 (1982).

[20] H. Albrecht, *et al.*, Z. Phys. C **48**, 543 (1990).

[21] W-M Yao *et al*, J. Phys. G: Nucl. Part. Phys., **33** 1 (2006).

[22] Heavy Flavor Averaging Group (HFAG), 0704.3575[hep-ex].

[23] M. Pivk and F. R. Le Diberder, Nucl. Instrum. Meth. A **555** 356 (2005).